

See discussions, stats, and author profiles for this publication at: <https://www.researchgate.net/publication/51466504>

A Biomimetic Approach to Enhancing Interfacial Interactions: Polydopamine-Coated Clay as Reinforcement for Epoxy Resin

ARTICLE *in* ACS APPLIED MATERIALS & INTERFACES · JULY 2011

Impact Factor: 6.72 · DOI: 10.1021/am200532j · Source: PubMed

CITATIONS

73

READS

133

7 AUTHORS, INCLUDING:



Liping Yang

Institute of Chemical and Engineering Sciences

41 PUBLICATIONS 918 CITATIONS

SEE PROFILE



Jun Kai Herman Teo

DKSH Management Ltd./DKSH Holding Ltd

5 PUBLICATIONS 148 CITATIONS


SEE PROFILE

A Biomimetic Approach to Enhancing Interfacial Interactions: Polydopamine-Coated Clay as Reinforcement for Epoxy Resin

Liping Yang,[†] Si Lei Phua,[†] Jun Kai Herman Teo,[†] Cher Ling Toh,[†] Soo Khim Lau,[‡] Jan Ma,[†] and Xuehong Lu^{*,†}

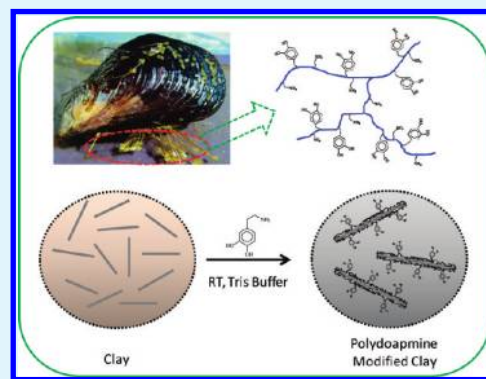
[†]School of Materials Science and Engineering, Nanyang Technological University, Singapore 639798, Republic of Singapore

[‡]Singapore Institute of Manufacturing Technology, 71 Nanyang Drive, Singapore 638075

 Supporting Information

ABSTRACT: A facile biomimetic method was developed to enhance the interfacial interaction in polymer-layered silicate nanocomposites. By mimicking mussel adhesive proteins, a monolayer of polydopamine was constructed on clay surface by a controllable coating method. The modified clay (D-clay) was incorporated into an epoxy resin, it is found that the strong interfacial interactions brought by the polydopamine benefits not only the dispersion of the D-clay in the epoxy but also the effective interfacial stress transfer, leading to greatly improved thermomechanical properties at very low inorganic loadings. Rheological and infrared spectroscopic studies show that the interfacial interactions between the D-clay and epoxy are dominated by the hydrogen bonds between the catechol-enriched polydopamine and the epoxy.

KEYWORDS: biomimetics, dopamine, clay, nanocomposite, interface



INTRODUCTION

Polymer nanocomposites containing low volume fractions of clay, i.e., layered silicates, frequently exhibit significantly improved properties over the corresponding neat polymers. Among the myriad factors that ultimately influence the global properties of polymer/clay nanocomposites, filler dispersion and interfacial interactions are the most crucial ones affecting the mechanical properties of the nanocomposites.^{1–5} For optimal properties, the platelets should be well-dispersed in the matrices to obtain a high aspect ratio and large interfacial area between the phases, whereas strong interfacial interactions between the clay and matrices would facilitate the stress transfer from the matrices to the clay. Because nanosized clay has an extremely high surface area to volume ratio, in a nanocomposite system with strong interfacial interactions, a very small amount of clay may have the potential to significantly improve the stiffness of the material.

The most established method to improve clay dispersion in polymers is to modify the clay surface with organic surfactants via cationic exchange procedures. The attachment of surfactants on clay surface leads to the expansion of clay interlayer galleries, facilitating clay exfoliation and making clay more compatible with organic polymers.^{6–13} However, the main interfacial interactions between the organoclay and polymer matrices are van der Waals interactions,^{14–17} which are weak interactions inferior in stress transfer compared with covalent or hydrogen bonds.

A common strategy to enhance the interfacial interactions in polymer/clay nanocomposites is to prepare the nanocomposites via in situ polymerization in the presence of functional coupling agents, such as silane coupling agents containing hydroxyl, carboxyl, epoxy or amine groups. It is believed that the silane

group could react with hydroxylated edge of clay platelets while those active amine, carboxyl, epoxy or hydroxyl groups afforded the possibility of the reaction with polymer matrix.^{18–21} The amount of hydroxyl groups on clay edge is, however, very small, and the reactions require strict chemical conditions. Furthermore, the main caveat of this strategy is that the coupling agents are often material-specific, and thus lack efficacy across a broad range of polymer matrices. To surmount these problems, a more generic clay-functionalization strategy has to be formulated to create strong interactions between clay and a wide variety of polymer matrices for property improvements.

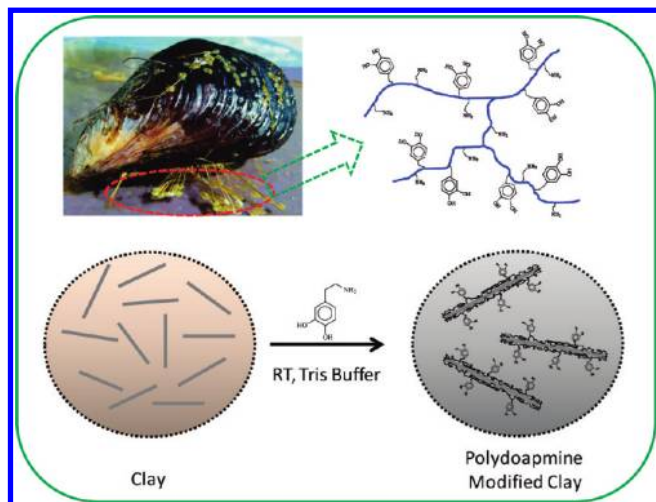
Recently, marine mussel adhesive proteins (MAPs) have attracted great attention owing to the amazing ability of mussels to adhere to various kinds of surfaces.^{22,23} The MAPs contain large amounts of a particular amino acid known as 3,4-dihydroxy-L-phenylalanine (dopamine, DOPA), which is found at high concentrations at the adhesive interfaces between the mussels and substrates. Previous research work has shown that the catechol groups in DOPA are capable of forming hydrogen bonds, metal–ligand complexes, and quinhydrone charge-transfer complexes, which afford the mussels with strong adhesion to various types of materials.^{24–26} In 2007, Lee et al. reported polydopamine (PDOPA) adhesive coatings on a wide variety of material surfaces including noble metals, oxides, polymers, semiconductors and ceramics prepared by mimicking MAPs.²² Podsiadlo et al. reported nacre-like materials prepared via layer-by-layer

Received: April 30, 2011

Accepted: July 5, 2011

Published: July 05, 2011

Scheme 1. Schematic Illustration of Surface Coating of Na-MMT with Polydopamine by Mimicking Mussel Adhesive Proteins



assembly of clay and DOPA-Lys-PEG copolymers, in which DOPA units were found to impart excellent mechanical properties to the composite.²⁷ Inspired by these work, we hypothesized that if a catechol-rich polymer layer can be prepared as the interface between clay and polymers, the interfacial interactions may be significantly enhanced and hence the stiffness of the nanocomposites can be improved significantly at very low clay loadings owing to the more effective stress transfer. To verify the hypothesis, we prepared dopamine-modified clay (D-clay) via a facile water-assisted process and incorporated the D-clay into an epoxy resin to form nanocomposites. Herein, we report the structure, morphology, and thermomechanical properties of these novel materials.

EXPERIMENTAL SECTION

Materials. Pristine montmorillonite clay (Na-MMT) with cationic exchange capacity of 145 mmol/100 g was obtained from Nanocor Inc. Organoclay Cloisite 93A was purchased from Southern Clay Corp. Epoxy precursor DER 332 and amine hardener Ethacure-100LC were supplied by Dow Chemicals and Albemarle Corp, respectively. 3,4-Dihydroxyphenethylamine hydrochloride (DOPA, 98%), tris(hydroxymethyl)aminomethane (TRIS, 99%) and acetone were purchased from Aldrich and used as received.

Sample Preparation. In a typical experiment, Na-MMT (1 g) was mechanically stirred in 100 mL of deionized water for 24 h, followed by rest at room ambient for 2 days. After removing the precipitate, the suspension was poured into 250 mL 10 mM TRIS buffer solution (pH 8.5).²² DOPA (0.55 g) was then added and the suspension was stirred for 2 h at room ambient. The suspension was then centrifuged at 7500 rpm for 20 min. Similar to those reported solvent exchange methods,^{28–31} the dark slurry-like product was washed with acetone, and the solvent was removed by centrifuge. The wash-centrifuge step was repeated four times, and finally the obtained D-clay/acetone slurry was redispersed in 200 mL of analytical reagent grade acetone. PDOPA was prepared as a reference by self-polymerization of DOPA without MMT for 60 h in Tris buffer, the solid product collected from the Tris buffer were filtered and then washed by DI water for at least 5 times. The dark coffee-like powder was obtained after drying in a vacuum oven at 50 °C for 48 h. To prepare the epoxy/D-clay nanocomposites, a certain

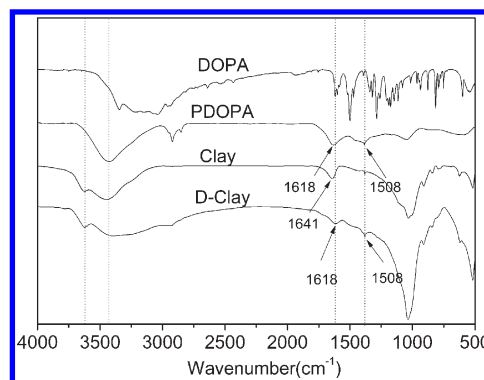


Figure 1. FTIR spectra of DOPA, PDOPA, pristine clay (Na-MMT), and D-clay.

amount of DER 332 was poured into the slurry followed by vigorous stirring for 2 h. The acetone was then removed by rotary evaporation followed by drying in a vacuum oven at 50 °C for 48 h. The curing agent was then added at the epoxy/curing agent ratio of 3.8/1 (w/w). The mixtures were mechanically stirred for 30 min, degassed at 50 °C, and cured at 100 °C for 2 h and postcured at 180 °C for 5 h. An epoxy/Na-MMT nanocomposite was prepared as a reference using the same procedure except that the clay was not treated with DOPA. An epoxy/organoclay nanocomposite was also prepared by mechanically mixing the epoxy and Cloisite 93A at 75 °C and 800 rpm for 120 min. After being mixed with curing agent, the mixture was degassed and cured as described above. The inorganic loadings of the D-clay/epoxy nanocomposites determined via thermogravimetric analysis (TGA) are 0.9, 1.4, and 3.5 wt %, respectively, whereas that of the epoxy/Na-MMT and epoxy/organoclay are 3.9 and 3.4 wt %, respectively.

Characterization. X-ray photoelectron spectroscopy (XPS) measurements were conducted on a Kratos Analytical AXIS His spectrometer with a monochromatized Al K α X-ray source (1486.6 eV photons). For TGA,³² Fourier transform infrared (FTIR) spectroscopy,³³ wide-angle X-ray diffraction (WAXD),³³ transmission electron microscopy (TEM),³³ and dynamic mechanical analysis (DMA)³⁴ studies, the instruments and measurement conditions were the same as those reported in the aforementioned references. For atomic force microscopic (AFM) studies, the D-clay suspensions were cast onto a silica wafer and dried at room temperature. Tapping mode AFM images were obtained at ambient conditions using a Dimension 3100 AFM (Digital Instruments) with Si tips. The viscosity of the epoxy/D-clay precursors was measured at constant shear rate in the temperature range of 25 to 140 °C using a cone–plate rheometer of 25 mm in diameter (TA Instruments AR1000N) with controlled stress. Before each temperature-sweep experiment, preshear was performed at the shear rate of 10 s^{−1} for 5 min, followed by a 60 min resting time.

RESULTS AND DISCUSSION

Biomimetic Surface Modification of MMT by Polydopamine. We prepared catechol-rich coats on MMT via surface polymerization of DOPA by mimicking MAPs (Scheme 1). After DOPA was added into the clay suspension in TRIS buffer, the color of the suspension turned into pink in several minutes owing to the oxidation of the catechol of dopamine to dopaminequinone.³⁵ The resultant dopaminequinone were then involved in a series of redox isomerizations and oxidations, and some of these “monomers” finally “polymerized” onto clay surface, leading to the dark coffee color of the D-clay (see Figure S1 in the Supporting Information). The successful coating of PDOPA on MMT surface is verified by XPS (see Figure S2 in the Supporting

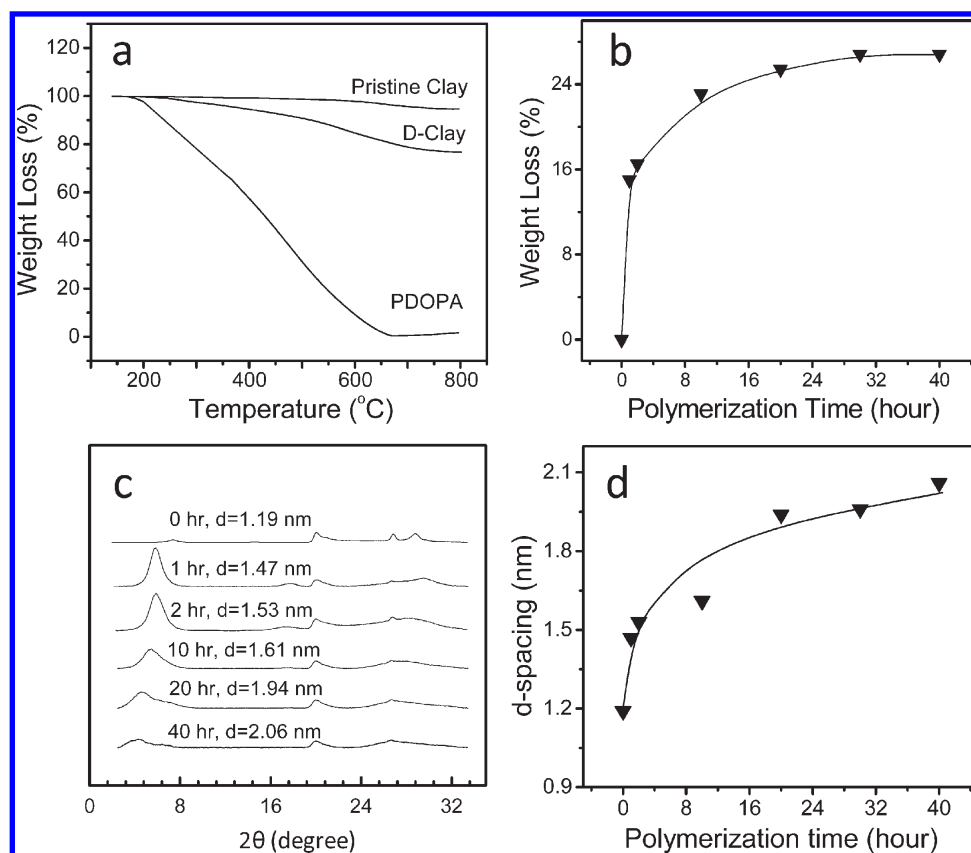


Figure 2. (a) TGA curves of Na-MMT, PDOPA, and D-clay in air. (b) Weight loss of D-clay as a function of DOPA polymerization time. (c) WAXD patterns of D-clay obtained at different polymerization time. The intensities of the peaks are normalized according to the quartz peak at $2\theta = 20^\circ$ found in Na-MMT. (d) The d -spacing of the D-clay as a function of polymerization time. For all, the D-clay was prepared at DOPA concentration of 1.5 mg/mL.

Information). For the pristine clay, intrinsic oxygen, sodium and silicon atoms are detected by XPS. After coating with PDOPA, the signal from sodium atoms disappears completely, and that from oxygen and silicon are largely weakened. Instead, greater amounts of carbon and considerable amount of nitrogen are detected. FTIR spectra of the DOPA, PDOPA, pristine clay, and D-clay are shown in Figure 1. The identical bands found for PDOPA and D-clay further confirm that DOPA has been polymerized into PDOPA on MMT.³⁶

Because the clay may catalyze the polymerization of DOPA³⁵ and the growth of PDOPA on oxides depends on the presence of nonoxidized dopamine molecules in the system,³⁷ the conversion of DOPA to the PDOPA coating on clay could be well-controlled by adjusting DOPA concentration and polymerization time. We used TGA to monitor the amount of PDOPA coated on clay. A typical TGA curve of the D-clay is shown in Figure 2a, on which the weight loss between 230 and 650 °C can be ascribed to the degradation of PDOPA.³⁶ Based on the TGA results, at a low DOPA concentration (0.1 mg/mL), almost all DOPA molecules can be converted into the PDOPA coating within four hours, whereas at a much higher concentration (1.5 mg/mL), the conversion is only about 40% in four hours (see Figure S3 in the Supporting Information). In the latter case, the conversion rate starts to slow down after two hours of polymerization (Figure 2b). It implies that once the clay surface is almost covered by a monolayer of PDOPA, the surface polymerization slows down.³⁸

The above claim is strongly supported by the results of our WAXD studies. Figure 2c shows that the d -spacing of Na-MMT

is about 1.19 nm. After polymerization for one hour, the D-clay shows a narrow peak at $2\theta = 6.02^\circ$, corresponding to d -spacing of 1.47 nm. Considering that DOPA is able to polymerize on both sides of a clay platelet, the thickness of the PDOPA coating is only about 0.14 nm on each side. From this, it can be easily deduced that a monolayer of PDOPA is coated on clay with its rings parallel to the clay surface. With two hours of polymerization, the d -spacing is increased to only 1.53 nm, indicating that the clay surface is still mainly covered by a monolayer at this stage. After 2 h of polymerization, the basal d -spacing of D-clay increases much more slowly (Figure 2d), and the (001) peak becomes weaker and broader (Figure 2c), indicating that the D-clay platelets are more difficult to aggregate to form regular stacks. After 40 h of polymerization, the (001) peak becomes very weak and broad, implying that at this stage most of the D-clay platelets do not aggregate into regular stacks even at solid state. Probably, with the progress of dopamine polymerization, some PDOPA colloidal particles are formed in the suspension. Because of the undifferentiated surfaces of PDOPA colloidal particles and D-clay platelets, these colloidal particles are very difficult to be separated from the D-clay, they are inclined to form irregular aggregates with D-clay platelets. Indeed, TEM results (see Figure S4 in the Supporting Information) show that some D-clay platelets stack together to form thin tactoids, while the thin tactoids are standing or laying on the TEM grids in a disordered manner. AFM images give further evidence to support the conclusion, as shown in Figure S5 in the Supporting Information. The surface of the D-clay obtained after 2 h of polymerization is

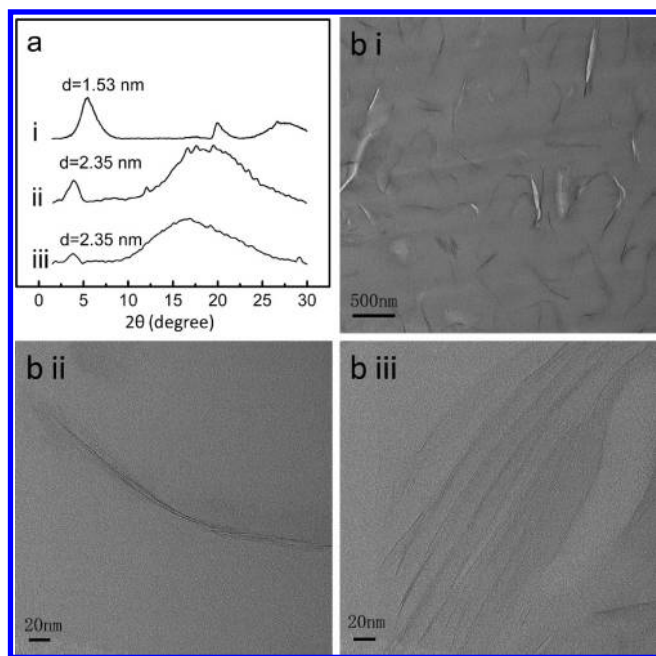


Figure 3. (a) WAXD patterns of (i) the D-clay, (ii) epoxy/D-clay precursor, and (iii) epoxy/D-clay nanocomposite. The D-clay was prepared with 2 h polymerization time. The inorganic loading of the epoxy/D-clay is 3.5 wt %. (b) TEM images of the epoxy/D-clay nanocomposite with 1.4 wt % inorganic content showing (i) typical overall morphology, (ii) a typical clay tactoid, and (iii) some exfoliated clay layers.

smooth, and the thickness of the platelet is about 3.2 nm, whereas for the D-clay obtained after 48 h of polymerization the surface is fairly rough, and the thickness is increased to more than 8 nm, demonstrating the presence of PDOPA colloidal particles on the surface.

Morphology and Properties of Epoxy/D-clay Nanocomposites. Although the D-clay with thick PDOPA coating has more disordered structure, the presence of PDOPA colloidal particles attached to the D-clay platelets is undesirable for being used as reinforcement, hence the D-clay with 2 h polymerization is used for nanocomposite fabrication. In order to keep the D-clay with a monolayer of PDOPA at disordered state, the D-clay slurry in acetone was used to mix with the epoxy. From the WAXD patterns shown in Figure 3a, we can see that the d -spacing of the D-clay is expanded from 1.53 to 2.35 nm after mixing with the epoxy monomer, indicating the intercalation of the D-clay by the monomer. After curing, the peak at $2\theta = 3.8^\circ$ is significantly weakened, implying partial exfoliation of the D-clay during the cure. TEM studies show that in the cured nanocomposites, most of the D-clay platelets are in the form of thin tactoids consisting of only a few layers and they are randomly dispersed in the matrix (Figure 3bi). The thickness of the tactoids is around 10 nm and the average length-to-thickness ratio is about 50 (Figure 3bii). Exfoliated single layers can also be observed in the dark roridous area near the tactoids (Figure 3biii), implying that some D-clay platelets were peeled off from the intercalated tactoids during the cure, which is consistent to the WAXD results. In contrast, much thicker tactoids are observed in the epoxy/Na-MMT nanocomposite prepared using a similar procedure (Figure 4a,b) as well as in the epoxy/organoclay nanocomposite (Figure 4c,d). The above results demonstrate that the PDOPA coating on the clay surface greatly benefit the

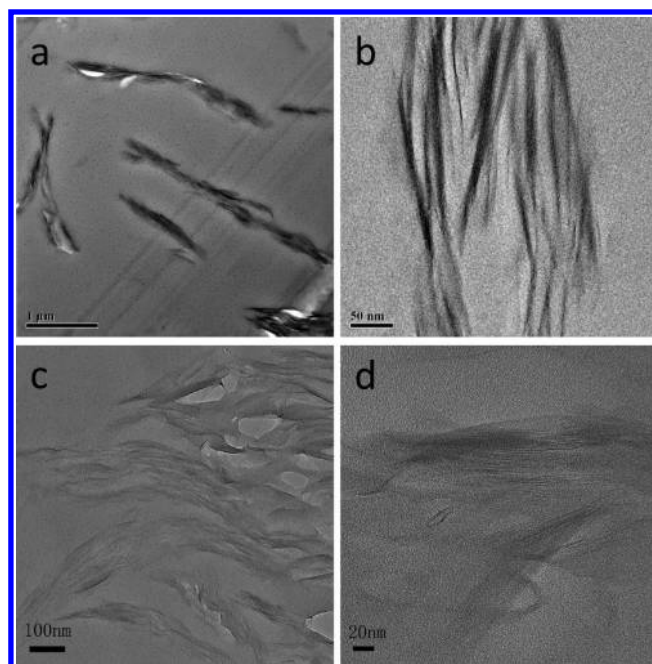


Figure 4. TEM images of (a, b) the Na-MMT/epoxy nanocomposite with 3.9 wt % inorganic content and (c, d) organoclay/epoxy nanocomposite with 3.4 wt % inorganic content.

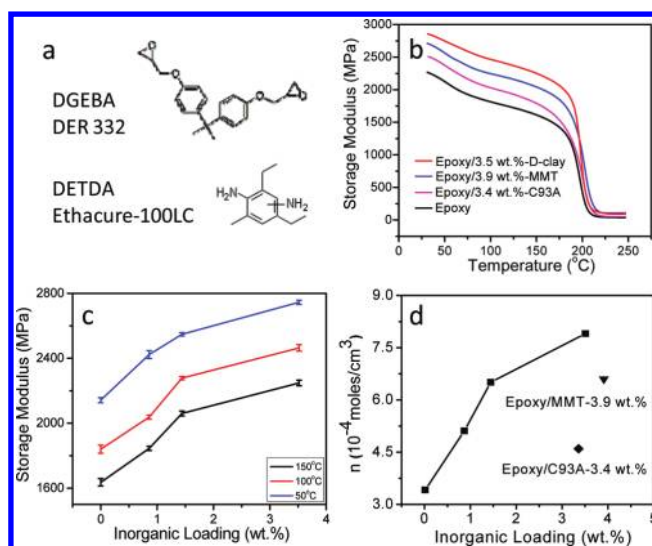


Figure 5. (a) Chemical structures of the epoxy and amine hardener. (b) Typical DMA curves of the neat epoxy resin, the D-clay/epoxy, Na-MMT/epoxy, and organoclay/epoxy nanocomposites with similar inorganic loadings (see labels). (c) Storage moduli of the D-clay/epoxy nanocomposites at different temperatures as a function of inorganic loading. (d) Number of active network chain segments per unit volume (n) in the D-clay/epoxy nanocomposites as a function of inorganic loading.

intercalation and exfoliation of D-clay in epoxy because of its stronger interactions with the matrix.

The structures of the epoxy precursor and amine hardener used in this work are given in Figure 5a. The incorporation of the D-clay into the epoxy resin brings about impressive enhancement in storage modulus (E') over that of the neat epoxy resin at low clay loadings; the increase in modulus is up to 30% at 3.5 wt %

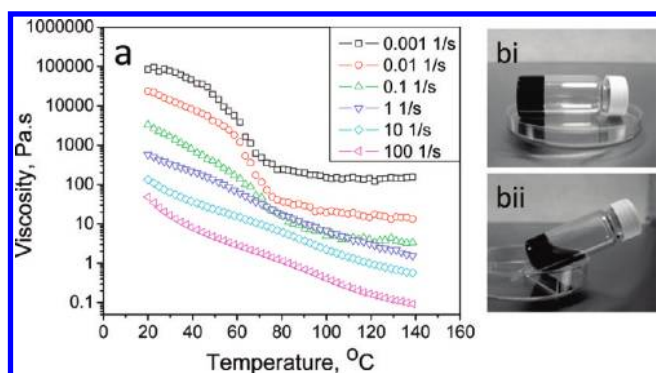


Figure 6. (a) Viscosity of the D-clay/epoxy precursor as a function of temperature under constant shear rate; (b) unique rheological behavior of the D-clay/epoxy precursor with 1 wt % D-clay (i) before and (ii) after mixing with the hardener.

inorganic loading (Figure 5b). The reinforcing effect of D-clay is clearly much more impressive than that of pristine clay and organoclay. For example, at 50 °C, the modulus enhancement brought by the addition of the D-clay at 1.4 wt % inorganic loading is comparable to that of pristine clay at 3.9 wt % inorganic loading and much higher than that of organoclay at 3.4 wt % inorganic loading (Figure 5b,c). The reinforcement effect is more sensitive to the clay loading when the inorganic loading is less than 2 wt % (Figure 5c), probably because of the better dispersion at low clay contents. Some prior work on epoxy/clay also showed ~30% increase in E' upon the addition of 5.0 wt % S-clay, which is based on the edge modification of clay using silane coupling agents with amine groups that could form covalent bonds with epoxy matrix.^{29,30} The reinforcement effect of the D-clay is even slightly stronger than that achieved with the fully covalent-bond approach.

In epoxy/clay nanocomposites, chemical cross-linking may be blocked by clay platelets to some extent.³³ However, if interfacial interactions are strong, clay may act as physical cross-linkers. To demonstrate this effect, we estimated the apparent number of active network chain segments per unit volume (n) using the classical rubber elasticity equation:³⁹

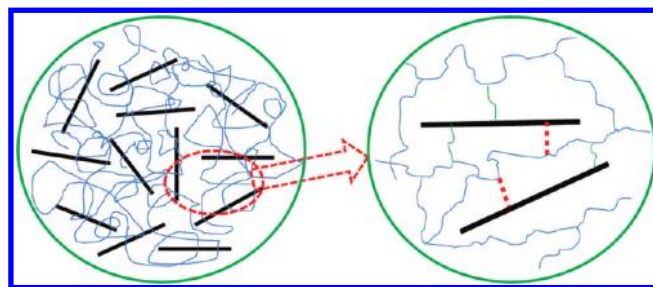
$$E = 3nRT \quad (1)$$

where E is the E' at the onset of the rubbery plateau, R the gas constant, and T the absolute temperature where the E' is located. Figure 5d shows that n increases with the D-clay loading, and at similar inorganic loadings, n for the epoxy/D-clay system is much larger than that of the epoxy/Na-MMT and epoxy/organoclay systems. It is not surprising that organoclay gives the lowest n , as van der Waals interactions would largely diminish at high temperatures. The above results signify the much stronger interfacial interactions in the epoxy/D-clay nanocomposites. n also increases with the inorganic loading more sharply when the inorganic loading is less than 2 wt %, which corroborates the trend observed for the glassy modulus.

Interfacial Interactions in Epoxy/D-clay Nanocomposites.

In this work, what interested us most is the interfacial interactions between the D-clay and the epoxy matrix. Pinnavaia et al. classified the main interfacial interactions between organoclay and a polymer into three types.¹⁴ Type A is the weak van der Waals interactions between the polymer and the alkyl chains of the onium ions, which are believed to be less important than type

Scheme 2. Schematic illustration of the Possible Interactions in Clay/Epoxy Nanocomposites: Dashed Line, Hydrogen bond; Solid Line, Covalent Bond



B, the binding interactions of the polymer with the siloxane basal surfaces. Type C is the binding of the hydroxylated edges of the silicate layer to the polymer. For the epoxy/C93A system, the main interfacial interaction is type A, which is weaker than the type B interactions in the epoxy/pristine clay system. As for the epoxy/D-clay system, since there are many catechol hydroxy groups on the surface of D-clay, the major interfacial interactions should be similar to type C interactions but they are much more prominent because the amount of catechol groups on clay surface is much larger than that of the hydroxyl groups on clay edge.

Evidence of the strong interactions between D-clay and the epoxy is the unique rheological behavior of the epoxy/D-clay precursor. The strong interactions of the D-clay with the epoxy monomer lead to gel-like behavior of the epoxy/D-clay precursor at very low D-clay loading (Figure 6bi). This is due to physical cross-linking caused by the hydrogen bonds between the epoxy molecules and D-clay, where the catechol groups act as proton donors, while the C—O—C groups in the epoxy act as proton acceptors. Upon mixing the D-clay/epoxy precursor with the amine hardener, the amine groups of the hardener compete with the catechol groups as proton donors. As the amount of the amine groups is much higher than that of the catechol groups, the amine groups will be the main proton-donors, whereas the C—O—C groups in the epoxy act as proton-acceptors. As a result, the gel is destroyed (Figure 6bii) as both the clay platelets and epoxy molecules may mainly interact with small amine molecules. When the viscosity of the D-clay/epoxy precursor was measured as a function of temperature under steady shear at a shear rate of lower than 1 1/s, a sharp viscosity drop could be observed between 60 and 80 °C (Figure 6a), and this transition is reversible. This also strongly supports that the main interactions between the D-clay and epoxy are likely to be hydrogen bonds. After curing, most amine hardener molecules become proton-acceptors again and there are also numerous C—O—C and OH groups in epoxy segments that can form hydrogen bonds with the catechol groups (Scheme 2).

Evidence for the hydrogen bonds between the catechol groups of the PDOPA layer and the clay surface as well as that between the catechol groups and the C—O—C groups in the epoxy molecules can also be found from the FTIR spectra of the D-clay, PDOPA/epoxy monomer mixture and neat PDOPA (see Figure S6 in the Supporting Information). For PDOPA, the broad absorption band from the hydrogen-bonded catechol groups is located at 3434 cm^{-1} . It shifts to 3400 and 3418 cm^{-1} for the D-clay and the mixture of PDOPA/epoxy monomer, respectively. In general, a lower wavenumber in FTIR indicates relatively stronger interactions. Thus the different downshifts imply that

the hydrogen bonds between the catechol groups and clay surface are stronger than that between the catechol groups of PDOPA and the C–O–C groups of the epoxy, whereas both of them are stronger than the interactions between the catechol groups themselves. Furthermore, the intensities of the bands corresponding to the hydrogen-bonded catechol groups decrease with temperature in the range of 25 to 150 °C, while the intensities can almost be fully recovered after cooling down, indicating that the hydrogen bonds are reversible. It is also interesting to note that the bands from the hydrogen bonds do not completely diminish even at 150 °C, which is much higher than the transition temperature obtained from the rheological study as the later is actually a synergistic effect of heat and shear force. It has been reported that as few as three or four DOPA residues interacting with an oxide surface form hyperstable hydrogen bonds that would eclipse the strength of a covalent bond.^{40–42} This may help us understand why the hydrogen bonds can survive at relatively high temperatures, and why the PDOPA layer can effectively transfer the stress from the matrix to the clay.

Although the presence of abundant catechol groups on the surface of the D-clay would certainly be a key factor for the greatly enhanced interfacial interactions, the possibility of interfacial covalent bonding cannot be completely rolled out. One possibility is that the amine groups of the hardener may link with the PDOPA layer on clay via Michael addition or Schiff base reaction. Another possibility is that some of the unconsumed amine groups of dopamine or imine groups of PDOPA may react with epoxy molecules and form covalent bonds. Because of the complex chemical structure of PDOPA and probably low contents of such bonds in the system, a comprehensive study using various chemical characterization tools and model compounds is necessary to confirm the presence and nature of the covalent bonds, which will be a subject for future study.

CONCLUSIONS

In summary, by mimicking MAPs, a monolayer of PDOPA has been successfully coated on clay platelets. The PDOPA coating greatly benefits the intercalation and exfoliation of clay as well as interfacial interactions, and hence leads to enhanced thermomechanical properties at very low inorganic loadings. We believe that this approach can be applied to nanocomposite systems with other inorganic fillers or polymer matrices as the catechol-enriched coating have strong interactions with a wide variety of materials. This would pave a new way to improve the properties of various polymer nanocomposites.

ASSOCIATED CONTENT

S Supporting Information. Digital photographs; XPS spectra; TEM; AFM images of D-clay; weight loss of D-clay and the conversion of dopamine to the polydopamine coating within 4 h polymerization as a function of dopamine concentration; FTIR spectra of PDOPA, D-clay, and the mixture of the PDOPA and epoxy monomer. This material is available free of charge via the Internet at <http://pubs.acs.org>.

AUTHOR INFORMATION

Corresponding Author

*E-mail: asxhlu@ntu.edu.sg.

ACKNOWLEDGMENT

This work was supported by Science and Engineering Research Council of the Agency for Science, Technology and Research (A*STAR) Singapore under Grant 092 137 0014.

REFERENCES

- (1) Lagaly, G. *Appl. Clay. Sci.* **1999**, *15*, 1–2.
- (2) Giannelis, E. P. *Adv. Mater.* **1996**, *8*, 29–35.
- (3) Ray, S. S.; Okamoto, M. *Prog. Polym. Sci.* **2003**, *28*, 1539–1641.
- (4) LeBaron, P. C.; Wang, Z.; Pinnavaia, T. J. *Appl. Clay. Sci.* **1999**, *15*, 11–29.
- (5) Zaman, I.; Le, Q. H.; Kuan, H. C.; Kawashima, N.; Luong, L.; Gerson, A.; Ma, J. *Polymer* **2011**, *52*, 497–504.
- (6) Messersmith, P. B.; Giannelis, E. P. *Chem. Mater.* **1994**, *6*, 1719–1725.
- (7) Kawasumi, M.; Hasegawa, N.; Kato, M.; Usuki, A.; Okada, A. *Macromolecules* **1997**, *30*, 6333–6338.
- (8) Ma, J.; Yu, Z. Z.; Zhang, Q. X.; Xie, X. L.; Mai, Y. W.; Luck, I. *Chem. Mater.* **2004**, *16*, 757–759.
- (9) Kong, D.; Park, C. E. *Chem. Mater.* **2003**, *15*, 419–424.
- (10) Park, J. H.; Jana, S. C. *Macromolecules* **2003**, *36*, 2758–2768.
- (11) Becker, O.; Cheng, Y. B.; Varley, R. J.; Simon, G. P. *Macromolecules* **2003**, *36*, 1616–1625.
- (12) Zilg, C.; Mulhaupt, R.; Finter, J. J. *Macromol. Chem. Phys.* **1999**, *200*, 661–670.
- (13) Becker, O.; Varley, R. J.; Simon, G. P. *Polymer* **2002**, *43*, 4365–4373.
- (14) Shi, H. Z.; Lan, T.; Pinnavaia, T. J. *Chem. Mater.* **1996**, *8*, 1584–1587.
- (15) Wang, M. S.; Pinnavaia, T. J. *Chem. Mater.* **1994**, *6*, 468–474.
- (16) Lan, T.; Pinnavaia, T. J. *Chem. Mater.* **1994**, *6*, 2216–2219.
- (17) Lan, T.; Kaviratna, P. D.; Pinnavaia, T. J. *Chem. Mater.* **1995**, *7*, 2144–2150.
- (18) Herrera, N. N.; Letoffe, J. M.; Reymond, J. P.; Lami, E. B. *J. Mater. Chem.* **2005**, *15*, 863–871.
- (19) Wheeler, P. A.; Wang, J. Z.; Baker, J.; Mathias, L. J. *Chem. Mater.* **2005**, *17*, 3012–3018.
- (20) Carrado, K. A.; Xu, L. Q.; Csencsits, R.; Muntean, J. V. *Chem. Mater.* **2001**, *13*, 3766–3773.
- (21) Herrera, N. N.; Letoffe, J. M.; Putaux, J. L.; David, L.; Lami, E. B. *Langmuir* **2004**, *20*, 1564–1571.
- (22) Lee, H.; Dellatore, S. M.; Miller, W. M.; Messersmith, P. B. *Science* **2007**, *318*, 426–430.
- (23) Lee, H.; Lee, B. P.; Messersmith, P. B. *Nature* **2007**, *448*, 338–341.
- (24) Waite, J. H.; Tanzer, M. L. *Science* **1981**, *212*, 1038–1040.
- (25) Waite, J. H. *Int. J. Adhes. Adhes.* **1987**, *7*, 9–14.
- (26) Yu, M.; Hwang, J.; Deming, T. J. *J. Am. Chem. Soc.* **1999**, *121*, 5825–5826.
- (27) Podsiadlo, P.; Liu, Z. Q.; Paterson, D.; Messersmith, P. B.; Kotov, N. A. *Adv. Mater.* **2007**, *19*, 949–955.
- (28) Chen, B.; Liu, J.; Chen, H. B.; Wu, J. S. *Chem. Mater.* **2004**, *16*, 4864–4866.
- (29) Wang, K.; Wang, L.; Wu, J. S.; Chen, L.; He, C. B. *Langmuir* **2005**, *21*, 3613–3618.
- (30) Wang, K.; Chen, L.; Wu, J. S.; Toh, M.; He, C. B.; Yee, A. F. *Macromolecules* **2005**, *38*, 788–800.
- (31) Liff, S. M.; Kumar, N.; Mckinley, G. H. *Nat. Mater.* **2007**, *6*, 76–83.
- (32) Toh, C. L.; Xi, L. F.; Lau, S. K.; Pramoda, K. P.; Chua, Y. C.; Lu, X. H. *J. Phys. Chem. B* **2010**, *114*, 207–214.
- (33) Teo, J. K. H.; Toh, C. L.; Lu, X. H. *Polymer* **2011**, *52*, 1975–1982.
- (34) Teo, J. K. H.; Teo, K. C.; Pan, B. H.; Xiao, Y.; Lu, X. H. *Polymer* **2007**, *48*, 5671–5680.
- (35) Jaber, M.; Lambert, J. F. *J. Phys. Chem. Lett.* **2010**, *1*, 85–88.

- (36) Fei, B.; Qian, B. T.; Yang, Z. Y.; Wang, R. H.; Liu, W. C.; Mak, C. L.; Xin, J. H. *Carbon* **2008**, *46*, 1795–1797.
- (37) Bernsmann, F.; Ponche, A.; Ringwald, C.; Hemmerle, J.; Raya, J.; Bechinger, B.; Voegel, J. C.; Schaaf, P.; Ball, V. J. *Phys. Chem. C* **2009**, *113*, 8234–8242.
- (38) Cui, J.; Wang, Y.; Postma, A.; Hao, J.; Hosta-Rigau, L.; Caruso, F. *Adv. Funct. Mater.* **2010**, *20*, 1625–1631.
- (39) Jahromi, S.; Kuipers, W. A. G.; Norder, B.; Mijs, W. J. *Macromolecules* **1995**, *28*, 2201–2211.
- (40) Lee, H.; Scherer, N. F.; Messersmith, P. B. *Proc. Natl. Acad. Sci.* **2006**, *103*, 12999–13003.
- (41) Chirdon, W. M.; O'Brien, W. J.; Robertson, R. E. *J. Biomed. Mater. Res., Part. B* **2003**, *66B*, 532–538.
- (42) Zhao, H.; Robertson, N. B.; Jewhurst, S. A.; Waite, J. H. *J. Biol. Chem.* **2006**, *281*, 11090–11096.